

# MEASUREMENT OF DIAGNOSTICS RESPONSE BY RF PARAMETERS FOR HARD X-RAY LINE IN PAL-XFEL\*

H. Yang<sup>†</sup>, Pohang Accelerator Laboratory, 37673 Pohang, Korea

## Abstract

PAL-XFEL is a hard x-ray (HX) and soft x-ray (SX) FEL machine to generate 2.5 – 15 keV FEL in the HX line and 0.28 – 1.2 keV FEL in the SX line. The HX line consists of an e-gun, a laser heater, S-band accelerators, an X-band linearizer, three bunch compressors (BC), and a dog-leg line. PAL-XFEL maintains the stable operation and FEL delivery with more than 98% availability due to machine stabilities including RF modules. In order to investigate the stable operation, we measure the diagnostics response for bunch charge monitors, energy beam position monitors, bunch length monitors, and a FEL intensity with a photon beam position monitor by RF parameters - RF amplitude and phase for an e-gun, accelerators, and a linearizer. In this paper, we present mainly corresponding RF parameters for e-beam and FEL jitters by this measurement and matrix analysis.

## INTRODUCTION

PAL-XFEL is the third XFEL machine in the world using normal conducting linacs for e-beam accelerating. It is combined two lines - a Hard X-ray (HX) line generating 2.5 – 15 keV FEL and a soft x-ray (SX) line generating 0.28 – 1.2 keV FEL [1]. PAL-XFEL has been successfully operating and delivering XFEL since March 2017. The availability is more than 98% and the stability of beam parameters are under 0.02% for the e-beam energy, 7% for the peak current, and 10% for the FEL intensity. Especially, it has under 20 fs timing jitter - the most stable timing among XFEL machines in the world [2].

The HX line of PAL-XFEL consists of an e-gun, a Laser Heater (LH), S-band accelerators, an X-band Linearizer (XL), three Bunch Compressors (BC), and a Dog-Leg (DL) line (Fig. 1). The stable e-beam parameters are caused by the stability of RF devices in the injector and linac section, and magnet devices in bunch compressors and a dog-leg line. The stabilities from the error analysis with the ELE-GANT simulation are applied for RF and magnet devices in PAL-XFEL [3]. The required stability of the magnet power supply system is few ten's ppm and it is easy to achieve by the developed technology. However, some stabilities for RF devices are challenging, for example, 0.01° phase jitter for the injector RF device and 0.05° phase jitter for the X-band linearizer. Since we use the RF timing system, there is phase drift in all RF devices by the drift of reference timing.

In order to investigate and quantify effects of jitters, we measured diagnostics responses by RF parameters. Bunch Charge Monitors (BCM), Energy Beam Position Monitors (EBPM), Bunch Length Monitors (BLM), and a Quadratic photon Beam Position Monitor (QBPM) were used in this measurement. The FEL pulse energy can be obtained from

the sum value of the QBPM. The RF amplitude and phase of all RF modules were used. The response matrix was obtained from this measurement, and the main RF variables and modes for a FEL jitter were found by the method of Singular Value Decomposition (SVD) for the response matrix [4]

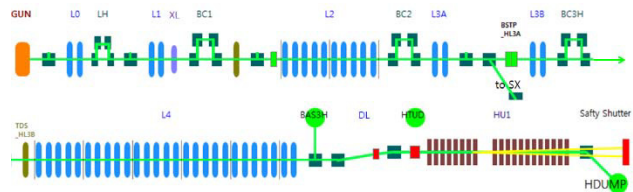


Figure 1: Layout of the HX line in PAL-XFEL.

## LATTICE AND INITIAL SETTING

The HX line in PAL-XFEL consists of an injector, the LH, 4 linac sections, 3 BCs, and the DL line. The injector include S-band photo-cathode RF e-gun and 2 linacs with individual RF modules (L0). Electron bunches are generated with the 5-ps bunch length and longitudinally Gaussian distribution in the gun. The e-beam are accelerated to 140 MeV at the end of the injector. The slice energy spread of e-beam are heated in the LH. The linac sections are divided by BCs. We call those as L1, L2, L3, L4, BC1, BC2, and BC3H (Fig. 1). The XL is located between L1 and BC1. 20 undulators and a self-seeding region are in HU1 section. The undulator K-value can be adjusted by moving the undulator gap, but we normally use fixed K-value of 1.87. We set the machine for 9.7 keV FEL generation in this measurement. The detail parameters are in Table 1 and 2.

Table 1: Beam Parameters for Initial Setting

Parameters	Value
Initial charge	248 pC
Final charge	185 pC
Bunch energy at LH	0.14 GeV
Bunch energy at BC1	0.35 GeV
Bunch energy at BC2	2.50 GeV
Bunch energy at BC3H	3.50 GeV
Final bunch energy	8.70 GeV
Initial peak current	20 A
Peak current after BC1	87 A
Peak current after BC2	390 A
Peak current after BC3H	2000 A
FEL energy	9.7 keV
FEL Pulse Energy	1.0 mJ

Table 2: RF and BC Parameters for Initial Setting

Parameters	Value
Gun RF phase	33.7°
L0_01 RF phase	0.00°
L0_02 RF phase	-2.00°
L1 RF phase	-11.05°
L2 RF phase	-20.85°
L3 RF phase	-10.50°
L4 RF phase	-2.00°
BC1 bunching angle	4.97°
BC2 bunching angle	3.00°
BC3H bunching angle	1.60°

The location and kind of diagnostics are in Fig. 2. An initial bunch charge was measured by BCM\_INI and a final bunch charge was measured by BCM\_FIN. We use collimator in the BC1, the final charge is about 75% of the initial charge. There are EBPMs and BLMs at each BC (EBPM\_BC1/BC2/BC3H and BLM\_BC1/BC2/BC3H). They are used to measure energies and bunch peak currents at BCs. All BLMs were calibrated by a bunch length measurement system with a transverse deflecting cavity. There are EBPMs at the LH, DL line and HDUMP. EBPM\_HDUMP were mainly used for measuring final e-beam energy in this measurement. The FEL pulse energy are measured by the QBPM in a HX beamline. It was calibrated by an energy-loss scanning method. The resolution of these diagnostics are in Table 3.

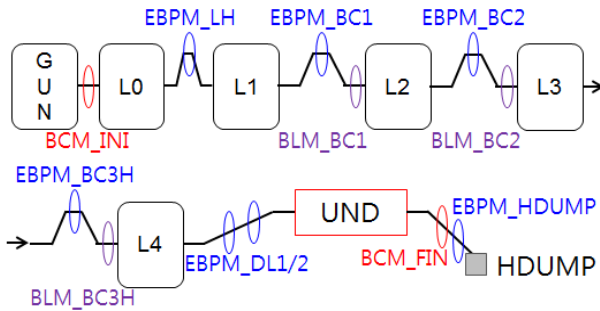


Figure 2: Diagnostics for HX in PAL-XFEL.

Table 3: Resolutions of Diagnostics

Diagnostics	Resolution
BCM_INI/FIN	0.1 pC
EBPM_LH	5.4 keV
EBPM_BC1	8.8 keV
EBPM_BC2	67.1 keV
EBPM_BC3H	168.8 keV
EBPM_HDUMP	85.5 keV
BLM_BC1	0.075 A
BLM_BC2	0.4 A
BLM_BC3H	5.0 A
QBPM (FEL pulse energy)	10 $\mu$ J

## DIAGNOSTICS RESPONSE

We measured the diagnostics response to refer the reference [4]. During this measurement, we varied the RF variables one by one. All diagnostics and RF variables read out bunch synchronously for each step. The RF variables were varied around initial setting and diagnostics measured over 20 points. We selected linear variation region of responses around initial values of variables and obtained the elements of a response matrix by the linear fitting. The diagnostics responses were divided by their resolutions (Table 3) and RF variations were divided by their sensitivities (Table 4). After measurement, we found that the diagnostics responses by the same kind of RF modules in linac sections are similar. Therefore, we present the response matrix classified by the sections for L1 – L4 in this paper.

Table 4: Resolutions of Diagnostics

RF module	Sensitivity
GUN RF phase	0.020°
S-band linac RF phase (L0 – L4)	0.020°
X-band linearizer RF phase	0.065°
Gun RF amp.	0.02%
S-band linac RF amp. (L0 – L4)	0.02%
X-band linearizer RF amp.	0.12%

Table 5 is the response matrix  $\mathbf{R}$ , where  $\Phi$  means the RF phase,  $A$  means the RF amplitude,  $C$  means the bunch charge,  $I$  means the peak current, and  $FEL\_EN$  means the FEL pulse energy. The bold numbers indicate the most influential RF variables for each diagnostics. For example, there is large response of the FEL pulse energy by  $\Phi_{XL}$ ,  $\Phi_{L1}$ ,  $\Phi_{GUN}$ . Since each diagnostics response on each RF variable is linear, this response matrix can be analysed by the method of SVD [5]. The response matrix  $\mathbf{R}$  is composed into three matrices according to

$$\mathbf{R} = \mathbf{U} \cdot \mathbf{S} \cdot \mathbf{V}^T, \quad (1)$$

where the matrix  $\mathbf{S}$  is a diagonal matrix containing the singular values of  $\mathbf{R}$ .  $\mathbf{S}$  is 11 by 11 matrix, but just 6 by 6 section were analysed here because of their larger singular values. The matrices of  $\mathbf{S}$ ,  $\mathbf{U}$ , and  $\mathbf{V}$  are in Table 6 – 8.

The mode #1 is related the final peak current and e-beam energy. The corresponding variables are mainly  $\Phi_{L1}$ ,  $\Phi_{XL}$ ,  $A_{L1}$ , and  $A_{XL}$ . The variation of e-beam energy at a BC changes the trajectory into the BC. Since it causes phase and energy gain variation of all RF modules after that BC, there are large response of the final energy and current by the RF modules before the first BC. The mode #2 is related to the final charge and FEL pulse energy. The corresponding variables are mainly  $\Phi_{L1}$  and  $\Phi_{XL}$ . Since, we collimate the e-beam at the center of BC1, the x-position, slice energy chirp, and linearization of bunch are related to the final charge. Since EBPM\_BC1 is less related to the mode #2, it can be inferred that mode #2 is acting on the linearization and slice energy chirp of bunch. The mode #3 is related to peak currents at BCs and final e-beam energy. The

main corresponding variables -  $\Phi_{L1}$ ,  $\Phi_{XL}$ , and  $A_{XL}$  - means that RF of L1 and XL affect the phase of the RF modules after BC1. The fourth mode is related to initial charge and the fifth mode is related to the e-beam energy at the injector. The sixth mode is related to the final charge and FEL pulse energy like mode #2, and  $A_{GUN}$ ,  $\Phi_{L1}$ , and  $\Phi_{L2}$  are main corresponding variables. Since the combination of  $\Phi_{L1}$  and  $\Phi_{L2}$  adjust the slice energy chirp, it can be concluded that mode #6 is acting on the slice energy spread.

Table 5: Response Matrix (R)

	$\Phi_{GUN}$	$\Phi_{L01}$	$\Phi_{L02}$	$\Phi_{L1}$	$\Phi_{XL}$	$\Phi_{L2}$	$\Phi_{L3}$	$\Phi_{L4}$
C_INI	1.35	0.33	0.03	-0.23	0.37	-0.08	-0.03	0.00
C_FIN	-1.05	0.61	0.92	3.51	-2.17	-0.14	-0.08	-0.01
EBPM_LH	0.66	-0.63	-0.12	-0.04	-0.01	0.01	0.00	0.01
EBPM_BC1	0.78	-0.05	-0.10	-0.95	-0.08	0.02	0.00	0.00
EBPM_BC2	-0.06	0.13	0.29	1.96	0.26	-0.52	0.00	0.02
EBPM_BC3H	0.01	0.07	0.13	0.87	0.11	-0.19	-0.10	0.01
I_BC1	-0.35	-0.30	-0.22	0.82	1.56	-0.03	-0.04	0.01
I_BC2	0.24	-0.51	-0.31	0.97	2.96	-0.48	0.00	0.03
I_BC3H	0.44	-0.17	0.66	2.95	2.98	-1.20	-0.03	0.06
EBPM_HD	-0.62	-0.19	-1.02	-6.58	-2.86	2.13	0.39	-0.17
FEL_EN	-0.97	0.33	0.21	1.12	-2.29	-0.20	-0.01	-0.01
	A_GUN	A_L01	A_L02	A_L1	A_XL	A_L2	A_L3	A_L4
C_INI	-0.06	0.06	-0.03	0.01	-0.62	0.01	0.03	0.02
C_FIN	-0.18	0.48	0.41	0.86	-1.02	-0.01	0.01	0.01
EBPM_LH	0.13	-0.32	-0.24	0.01	-0.05	0.00	0.00	0.00
EBPM_BC1	0.12	-0.15	-0.16	-0.29	0.33	0.00	0.00	0.00
EBPM_BC2	0.06	0.39	0.32	0.70	-0.84	-0.09	-0.01	0.00
EBPM_BC3H	0.02	0.17	0.14	0.31	-0.35	-0.03	-0.04	0.00
I_BC1	-0.07	0.21	0.19	0.43	-0.52	0.00	0.02	0.01
I_BC2	0.06	0.36	0.33	0.65	-0.83	-0.02	0.00	0.00
I_BC3H	0.09	0.95	0.87	1.65	-6.42	-0.05	-0.04	0.00
EBPM_HD	-0.30	-1.66	-1.47	-3.06	4.12	0.08	0.13	0.07
FEL_EN	0.38	0.10	0.16	0.30	0.75	0.00	0.01	0.00

Table 6: Matrix  $S$ , Containing the Singular Values of  $R$

	1	2	3	4	5	6	7	8
1	12.84	0.00	0.00	0.00	0.00	0.00	0.00	0.00
2	0.00	5.80	0.00	0.00	0.00	0.00	0.00	0.00
3	0.00	0.00	2.99	0.00	0.00	0.00	0.00	0.00
4	0.00	0.00	0.00	1.84	0.00	0.00	0.00	0.00
5	0.00	0.00	0.00	0.00	0.86	0.00	0.00	0.00
6	0.00	0.00	0.00	0.00	0.00	0.77	0.00	0.00
7	0.00	0.00	0.00	0.00	0.00	0.00	0.25	0.00
8	0.00	0.00	0.00	0.00	0.00	0.00	0.00	0.18

Table 7: Matrix U, Containing the First Six Left Singular Vector of  $R$  as Columns

	1	2	3	4	5	6
C_INI	-0.03	-0.15	-0.14	-0.63	-0.31	0.24
C_FIN	-0.19	0.67	-0.19	0.12	-0.03	0.57
EBPM_LH	0.01	-0.06	-0.01	-0.28	0.91	0.24
EBPM_BC1	0.07	-0.11	-0.06	-0.38	0.08	-0.14
EBPM_BC2	-0.17	0.15	0.10	-0.05	0.02	0.05
EBPM_BC3H	-0.08	0.06	0.05	-0.04	0.00	0.06
I_BC1	-0.12	-0.13	0.26	0.39	0.06	0.26
I_BC2	-0.19	-0.33	0.47	0.23	0.08	0.07
I_BC3H	-0.59	-0.32	-0.68	0.22	0.09	-0.12
EBPM_HD	0.72	-0.16	-0.42	0.33	0.06	0.18
FEL_EN	0.03	0.49	-0.03	0.07	0.21	-0.64

Table 8: Matrix V, Containing the First Six Right Singular Vector of  $R$  as Columns

	1	2	3	4	5	6
$\Phi_{GUN}$	-0.04	-0.27	-0.01	-0.93	0.07	0.20
$\Phi_{L0_01}$	0.00	0.15	-0.09	-0.14	-0.83	-0.06
$\Phi_{L0_02}$	-0.10	0.15	-0.13	-0.10	-0.16	0.08
$\Phi_{L1}$	-0.61	0.53	0.34	-0.04	0.14	0.34
$\Phi_{XL}$	-0.33	-0.73	0.48	0.21	-0.17	0.10
$\Phi_{L2}$	0.19	-0.01	-0.11	0.19	-0.04	0.62
$\Phi_{L3}$	0.03	-0.02	-0.05	0.07	0.03	0.01
$\Phi_{L4}$	-0.01	0.00	0.02	-0.02	0.00	-0.04
AGUN	-0.02	0.01	0.03	-0.07	0.26	-0.54
AL0_01	-0.16	0.05	0.07	-0.01	-0.33	-0.17
AL0_02	-0.14	0.05	0.06	0.03	-0.20	-0.24
AL1	-0.29	0.10	0.16	-0.08	0.08	-0.25
AXL	0.58	0.23	0.76	-0.11	-0.06	0.00
AL2	0.01	0.00	-0.01	0.01	-0.01	0.01
AL3	0.01	0.00	-0.01	0.01	-0.01	0.06
AL4	0.00	0.00	-0.01	0.01	0.00	0.03

## CONCLUSION

We measured diagnostics responses by RF variables - phase and amplitude of all RF modules. The initial and final charge, e-beam energy at LH, BC, and HDUMP, peak current after BCs, and FEL pulse energy read out bunch synchronously for each step of the RF variation in this measurement. The main RF variables for FEL and e-beam jitters were roughly found from the obtained response matrix, it was analysed by the method of SVD. The RF variables -  $\Phi_{L1}$  and  $\Phi_{XL}$  are mainly related to the variations of final e-beam energy, peak current, and FEL pulse energy. Also, we could classify the effect for the slice energy spread from XL, and the combination of L1 and L2 by this analysis.

## REFERENCES

- [1] I. S. Ko, *et al.*, Appl. Sci. **2017**, 7(5), 479.
- [2] H. S. Kang, *et al.*, Nature Photonics **11**, 708 (2017).
- [3] H. Yang, *et al.*, "Error Analysis for Linac Lattice of Hard X-ray FEL Line in PAL-XFEL," in *Proc. of FEL2014* (Basel, Switzerland, Aug. 25-29, 2014), p. 703.
- [4] F. Frei, *et al.*, "Experimental Results of Diagnostics for Longitudinal Phase Space," in *Proc. of FEL2014* (Basel, Switzerland, Aug. 25-29, 2014), p. 657.
- [5] D. Kalman, *A Singularly Valuable Decomposition: The SVD of a Matrix*, (The American University, Feb. 13, 2002).